Available online at www.sciencedirect.com
ScienceDirect
Biosensors and Bioelectronics 23 (2008) 1473–1480
BIOSENSORS & BIOELECTRONICS
www.elsevier.com/locate/bios

Microcavity array (MCA)-based biosensor chip for functional drug screening of 3D tissue models

Daniel Kloß [a], Randy Kurz [a], Heinz-Georg Jahnke [a], Michael Fischer [b], Andrée Rothermel [a], Ulf Anderegg [c], Jan C. Simon [c], Andrea A. Robitzki [a,*]

[a] *Center for Biotechnology and Biomedicine (BBZ), University of Leipzig, Division of Molecular Biological-Biochemical Processing Technology, Deutscher Platz 5, 04103 Leipzig, Germany*
[b] *Center for Innovation Competence, MacroNano® (ZIK), Institute for Micro- and Nanotechnologies (IMN), University of Ilmenau, Gustav-Kirchhoff-St. 7, 98693 Ilmenau, Germany*
[c] *Department of Dermatology, Venerology and Allergology, Leipzig University Medical Center, Philipp-Rosenthal-St. 23-25, 04103 Leipzig, Germany*

Received 14 August 2007; received in revised form 17 December 2007; accepted 3 January 2008
Available online 12 January 2008

Abstract

Multicellular tumour spheroids that mimic a native cellular environment are widely used as model systems for drug testing. To study drug effects on three-dimensional cultures in real-time we designed and fabricated a novel type of sensor chip for fast, non-destructive impedance spectroscopy and extracellular recording. Precultured spheroids are trapped between four gold electrodes. Fifteen individual 100 μm deep square microcavities with sizes from 200 to 400 μm allow an optimised positioning during the measurement.

Although apoptosis was induced in human melanoma spheroids by Camptothecin (CTT), treated cultures did not show disintegration but displayed increased impedance magnitudes compared to controls after 8 h resulting from an altered morphology of the outer cells. Contractions in cardiomyocyte spheroids were monitored when the innovative chip was used for recording of extracellular potentials. The silicon-based electrode array is used as an acute test system for the monitoring of any kind of 3D cell cultures. Since no adherence of cells or labelling is necessary the multifunctional sensor chip provides a basis for improved drug development by high content screenings with reduced costs and assay times. Additional improvements for parallel testing of different substances on one chip are presented.

Keywords: Monitoring; Microelectrode array; Tumour spheroids; Spheroid-based biosensor; Impedance spectroscopy

1. Introduction

One challenge for scientists working in the field of basic and applied pharmaceutical research is the development of biosensors for *in vitro* cell culture testing of physiological parameters under *in vivo*-like conditions. High content screening systems in drug development and validation processes have to be fast, labelling-free, if possible, and enable a non-destructive real-time monitoring of inter- and intracellular parameters without costly and time-consuming biological assays.

Spheroids were shown to be appropriate models for studying drug effects (Kunz-Schughart et al., 1998). The scaffold-free, rotation-mediated generation of sphere-like histotypic *in vitro* tissues (Thielecke et al., 2001; Reininger-Mack et al., 2002; Layer et al., 2002) can be applied to almost all primary cells of different donor tissues and cell lines by a self assembly process. Those multicellular spheroids, in contrast to commonly used monolayer cultures, are characterised by the formation of adequate cell–cell and cell–matrix contacts crucial for signal transduction and cellular communication to regulate fundamental cellular processes such as growth, proliferation, differentiation, migration and programmed cell death. Since they mimic the native three-dimensional cellular environment they better allow, for example, the monitoring of morphological alterations, penetration of drugs and/or cytotoxic agents then monolayers can. Therefore, spheroids represent excellent equivalents to non-vascularised *in vivo* microtumours of early stages. Also primary cardiac myocytes are

* Corresponding author. Tel.: +49 341 9731241; fax: +49 341 9731249.
E-mail address: andrea.robitzki@bbz.uni-leipzig.de (A.A. Robitzki).

0956-5663/$ – see front matter © 2008 Elsevier B.V. All rights reserved.
doi:10.1016/j.bios.2008.01.003

appropriate for creating *in vivo*-like contracting cardiomyocyte spheroids, since rotating cultivation of cardiac cells improves the formation of contractile filaments and a cellular syncytium. For impedance spectroscopy planar cell- and tissue-based biosensors with implemented microelectrodes have already been used to elucidate cellular electrical properties. However, effective screening devices for spheroid cultures are still missing.

Goal of this study was the development of a multielectrode array that allows fixation of suspended, not adhered, spheroids between multiple measurement electrodes. As established technologies in basic research and applied science impedance spectroscopy of tumour spheroids (e.g. mamma carcinoma, melanoma) and extracellular recording of electrically active spheroid cultures (neuronal cells, myocytes) are the main applications. In former studies cavities have proved to be appropriate for an easy and non-destructive trapping of spheres and subsequent isolation for further analysis. The range of typical spheroid sizes should be fully covered. So the fabrication of different geometries had to be realized on one array. Besides mechanical stability the sensor system was intended to be autoclavable, since no one-way device should be produced but a silicon-based multifunctional biosensor for long-term analyses especially with 3D cell cultures.

2. Materials and methods

2.1. Fabrication of the test system

The Sensor System Prototype was fabricated at the Center for Innovation Competence (University of Ilmenau, Germany). A 4-in. silicon wafer was chosen for an optimum yield of biosensor chips with the given dimension of the test system of 20 mm × 20 mm × 0.5 mm for each chip.

The mechanical fixing of the silicon chip in a carrier frame was realized by a precise silicone adhesion (Loctite 5366), which guarantees an excellent stability and tolerance at the demanded surrounding parameters (121 °C, 1 bar pressure, steam atmosphere, etc.). The electrical connection between silicon chip and carrier frame was accomplished by wire bonding. The silicon chip was fabricated using standard Micro-Electro-Mechanical Systems (MEMS) technologies (see Fig. 1d). First the 4 in. silicon wafer was structured by wet chemical anisotropic etching (etching speed depends on the crystal direction) in a 40% KOH solution at 90 °C. The cavity structure mapped in a chrome mask was transferred into the masking material (SiO_2) by a lithography step and a SiO_2-etching process (buffered HF solution). Due to the crystal orientation of the silicon (1 0 0) the square holes are etched under an angle of 54.7° into the substrate (like a pyramid stump). For a good electrical insulation of the con-

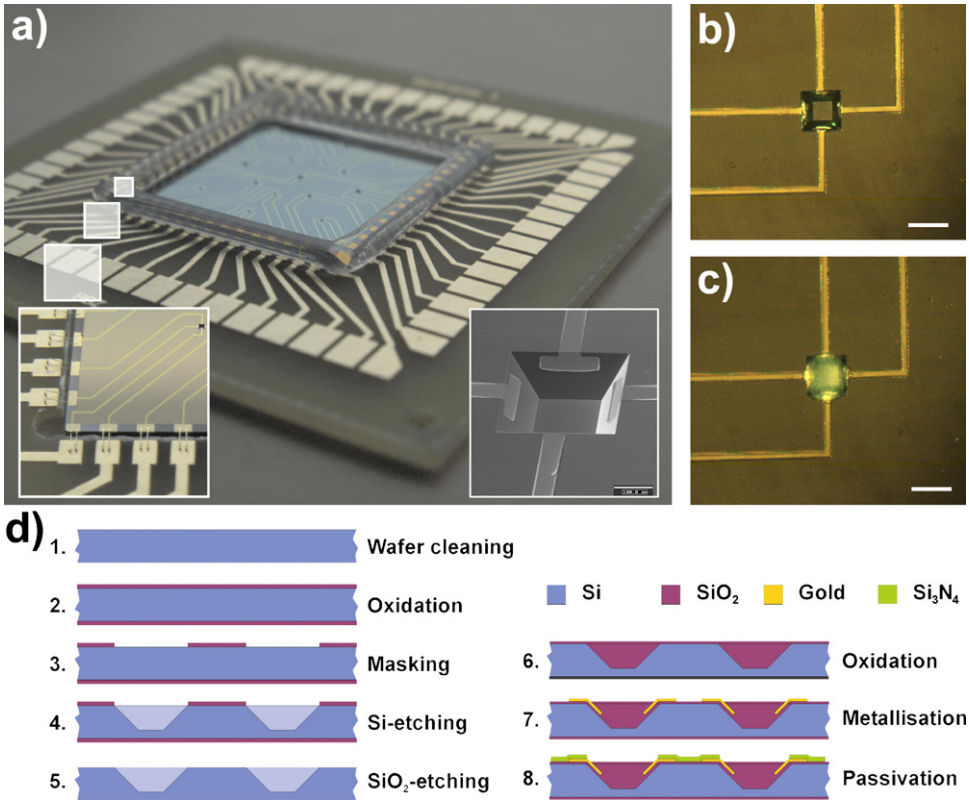

Fig. 1. Image and fabrication scheme of the silicon-based multielectrode biosensor. (a) Complete biosensor chip. Enlarged detail to the left: sealed bonds from the silicon inlet to the epoxy-glass resin frame with its 60 contact pads. Enlarged detail to the right: SEM micrograph of a square microcavity (200 μm × 200 μm) in the silicon substrate with four gold electrodes. (b and c) Light microscopy images of a single microcavity with and without a positioned spheroid (multicellular aggregate of human melanoma cells), bars = 200 μm. (d) Manufacturing steps: A 4 in. silicon wafer is structured by standard etching processes. Gold electrodes and conductors are sputtered onto a SiO_2 layer. The entire surface – except for the electrodes themselves – is finally passivated by Si_3N_4 for electrical insulation.

tacts which are produced subsequently, the wafer is oxidized thermally after structuring (O_2 atmosphere, 1050 °C) to obtain an 1800 nm SiO_2 coating over the complete wafer structure. The contact pads on the side wall of the cavities, as well as the chip conductor paths were realized with a lift off process. A specially thick resist layer (All Resist GmbH) allowing lithography on structured wafer surfaces was spin coated, exposed, and developed. Thereafter, a combined metal layer (10 nm titanium, 500 nm gold) was sputtered. After resist stripping, good quality side wall contact pads were obtained. For upward passivation a silicon nitride layer (700 nm) was deposited on the complete wafer surface by a plasma enhanced chemical vapour deposition (PECVD) process on a STS 310 (Surface Technology Systems Ltd.) at 350 °C with SiH_4 and NH_3. For cell connection it is necessary to bare the cavity contact pads and the bond pads from silicon nitride. This etching step was done by a reactive ion etching (RIE) process on a STS 320 (Surface Technology Systems Ltd.) with CHF_3 and CF_4 and a premanufactured resist mask. After batch processing the 4 in. wafer was sawed to obtain 12 silicon chips. In order to connect the silicon chips to an established measuring system a carrier system with milled cavities, gold-plated pads and circuit paths made of circuit board material (FR4) were developed. After wire bonding, the electrical junctions and the gap between chip and frame were sealed with silicone (Loctite 5366) by means of the commercial available dosing system dotmaster (DIMA SMT Systems). This kind of final passivation is leak proof and stress stable during all necessary cell cultivation operations. The complete biosensor chip comprised a silicon substrate with 15 square microcavities of three different sizes (200, 300, and 400 μm) and a uniform depth of 100 μm. The 60-electrode design was chosen to adapt it to a commercially available MEA measurement system (Multichannel Systems MCS GmbH, Reutlingen, Germany). All materials are biocompatible and resistant to heat (121 °C) and steam. Thus, the sensors can be cleaned and autoclaved easily. Mechanical stability and resistance to ethanol are important factors for multiple utilisation of the chips.

2.2. Cell culture

Bro (human melanoma) cells were cultured in a humidified atmosphere at 37 °C, 5% CO_2 in RPMI-medium supplemented with 10% fetal bovine serum, 2 mM glutamine and 0.2% penicillin/streptomycin (all supplied by Gibco). 10^6 cells (obtained by trypsinisation with 0.25% trypsin/EDTA, Gibco) were transferred to a cell culture dish with a hydrophobic surface containing 2 ml medium. Via constant rotation at 72 rpm (gyratory shaker) spheroids were formed after 24 h. Media were replaced every 2 days. To ensure working under sterile conditions in long time experiments a reservoir for cell culture medium and a lid can be fixed to the biosensor chip with silicone. Integrated holes in the lid allow an exchange of carbon dioxide or application of any substances. Cardiomyocytes isolated from neonatal (1 day old) Sprague–Dawley rats (preparation described in detail see Rothermel et al., 2005) were cultivated in DMEM-medium supplemented with 10% fetal bovine serum, 2 mM glutamine, penicillin (100 U/ml), streptomycin (100 μg/ml), gentamicin (20 μg/ml) and hydrocortisone (1 μg/ml) on a gyratory shaker as described above to form multicellular spheroids.

2.3. Impedance measurements

After 4 days of cultivation the tumour spheroids had achieved an average size of 250–400 μm. They were transferred onto the sensor chip. Measurements that did not take longer than 5–10 min (e.g. when measuring <25 spheroids) were done at room temperature without an additional medium reservoir. In this case the silicone packing frame on the chip was sufficient to accommodate up to 750 μl of culture medium. The sensor chip was placed in a measurement adapter and connected to an external impedance analyzer (Agilent 4294A). Exact positioning of spheroids into the cavities was done by a micropipette or a micromanipulator, and could be monitored via a light optical microscope. Thus, spheroids with diameters of about 270–350 μm were selected optically and sorted into a 300 μm microcavity. For comparison purposes this cavity and the same pair of electrodes were used for all experiments. Impedance spectra (magnitude and phase) were recorded at 100 mV (ac). A logarithmic sweep was performed within a frequency range of 1 kHz to 1 MHz with 10 points per decade and an averaging rate of five repeats for each frequency. Data were processed using Microsoft Excel and a self-written Visual Basic Script.

2.4. Extracellular recording

Chips were prepared for recording by coating the surface with 5 μg/ml laminin over night. When cardiomyocyte spheroids had achieved an average size of 180–250 μm after 4 days of cultivation they were transferred into a capable (200 μm) cavity on the sensor chip. Placed in a heated (∼37 °C) MEA1060 amplifier system (Multichannel Systems) recording of electric activity of the cardiomyocytes was carried out at a sampling rate of 4 kHz. Amplifier bandwidth was 0.1–10 kHz at a gain (factor) of 1200. A platinum wire was used as reference electrode. Data were processed and analyzed using MATLAB (The Mathworks, Natick, MA, USA) and Microsoft Excel with self-written Visual Basic Scripts.

2.5. Histochemistry

To induce apoptosis in melanoma cells, the precultured spheroids were treated with CTT (supplied by Sigma). CTT had been dissolved in DMSO (Merck) and was added to a final concentration of 1 μM after 4 days of cultivation. After incubation of 2, 4, 6, and 8 h spheroids were fixed with 4% PFA (paraformaldehyde in phosphate buffered saline, both supplied by Merck) for 30 min and stored in 25% sucrose at 4 °C. Cryosections (20 μm) were done with a Leica CM3050S microtome. Controls were treated with 1% DMSO only. To prove the induction of apoptosis, spheroid cryosections were incubated for 2 h with a caspase-3 antibody (rabbit anti-cleaved caspase-3, monoclonal, Cell Signaling). A red fluorescence con-

jugated secondary antibody (goat anti-rabbit IgG Cy3, Dianova) was used for detection. Nuclei were stained with Sytox green (Invitrogen). Photographs were taken using a confocal laser scanning microscope (Nikon TE2000). Counting the amount of caspase-3 positive cells and nuclei was carried out using the image processing software ImageJ (http://rsb.info.nih.gov/ij/). The characterisation of the cells as cardiac myocytes was done by staining with the muscle cell markers α-Actinin (mouse anti-alpha-Actinin, monoclonal, Sigma) and Desmin (rabbit anti-mDesmin, polyclonal, Dianova) and Cy2-conjugated secondary antibodies for fluorescence detection.

2.6. Statistics

Data represent the mean and standard deviation of caspase-3 staining for $n = 10$ cryosections and 3 series with $n = 25$ spheroids for each impedance experiment. To determine the significance of changes a Student's two-tailed t-test was performed for each point in time referred to the control (0 h). p-Values less than 0.05 were considered statistically significant.

3. Results

For the analysis of 3D spheroid cultures we designed and fabricated a microcavity array (MCA)-based sensor chip. The MCA consists of 15 square microcavities with widths of either 200, 300 or 400 μm and uniform depth of 100 μm. Rectangular gold electrodes are placed at the four sides of each cavity (Fig. 1). The chosen electrode configuration and the arrangement of the microcavities meet the basic requirements for positioning and electronic recording. This allows both the analysis of cellular parameters by impedance spectroscopy and the recording of extracellular field potentials for 3D cultures.

To validate the MCA-based sensor chip for (i) impedance spectroscopy of non-electrically active cells and (ii) extracellular recording of electrically active cells, tumour or cardiac spheroids were generated by using the cell culture technique mentioned before. In a first series of experiments we tested whether the MCA is suitable for measuring cellular alterations in tumour spheroids by means of impedance spectroscopy. The correct positioning of spheroids can be verified either by light microscopy (Fig. 1b and c) or more easily by comparing the recorded impedance spectra of covered versus non-covered electrodes in one cavity (Fig. 2a–c). The impedance remained unchanged at least for lower frequency ranges (Fig. 2a–c). When spheroids were exactly trapped between two pairs of electrodes, a detectable increase in impedance magnitude occurred in a frequency range of 10 kHz to 1 MHz. Pronounced impedance maxima of increased magnitudes for melanoma spheroids were found at 100–133 kHz. Phase angles ranged from −80° at 1 kHz to −20° at ∼250 kHz for a 400 μm cavity, and to −60° for a 200 μm microcavity (Fig. 2a–c). Differences in impedance magnitudes between (spheroid) "covered" and "uncovered" electrodes are significant for all cavity sizes in the characteristic frequency range around 100 kHz. For an "empty" 200 μm cavity $|Z|$ at 100 kHz is 19.6 kΩ, for 300 μm $|Z|$ is 6.8 kΩ, for a 400 μm cavity it is 5.1 kΩ.

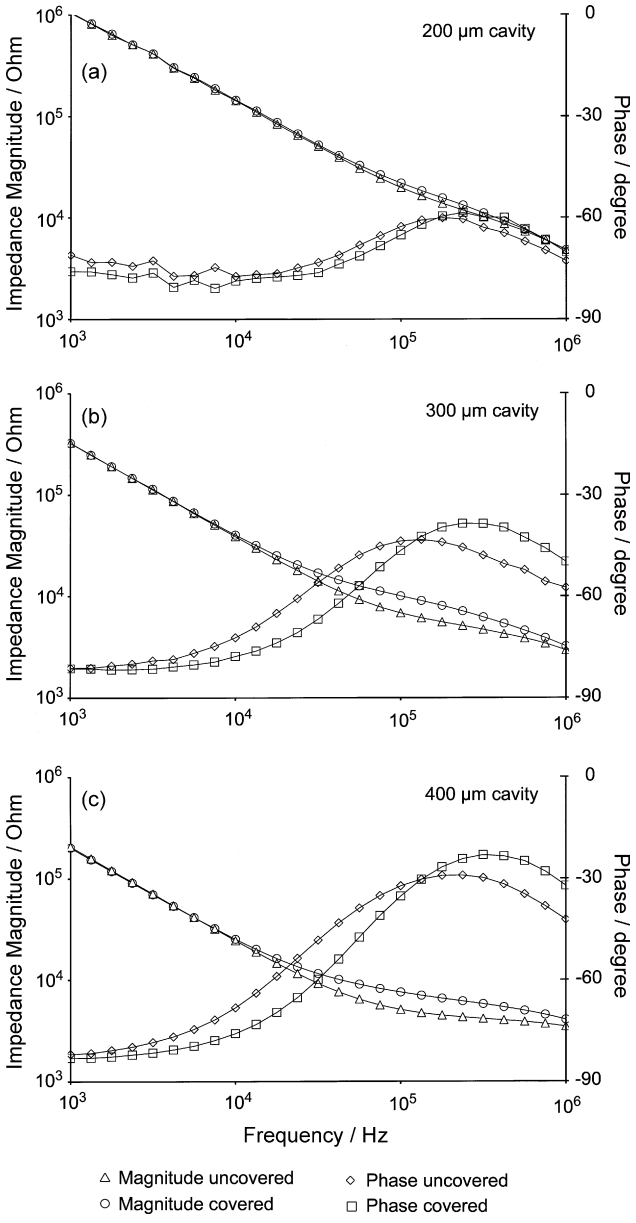

Fig. 2. Characteristic impedance spectra (magnitude and phase) of "uncovered" and (spheroid-) "covered" electrodes for all three sizes of microcavities in a frequency range from 1 kHz to 1 MHz. Impedance magnitudes decrease with higher frequencies and with increasing electrode area. "Covered" electrodes display higher impedance magnitudes above 10 kHz and shifted phase values. At around 100 kHz magnitudes are significantly higher for spheroid covered electrodes which is the basis for calculating the normalised impedance ΔZ.

For testing of drug-induced alteration by MCA-based impedance spectroscopy, human melanoma spheroids were precultured and transferred onto 300 μm cavities. Spheroids ranging from approximately 270 to 350 μm were analysed using the same pair of electrodes in all subsequent experiments. At day 4 one culture dish (initial number of cells: 1 million) contains about 185 spheroids with a typical diameter (77% of all spheroids) of 340 μm, 15% are smaller (>250 μm), 8% of the spheres achieve sizes of up to 500 μm. The average amount of cells in a 400-μm spheroid is approximately 10,000 at that

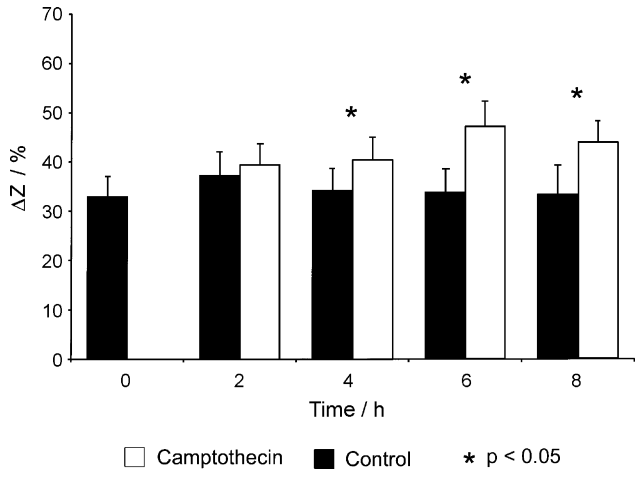

Fig. 3. Increased impedance alterations with progressive exposure time of human melanoma cells to Camptothecin (CTT). Spheroids were treated for 8 h, one set with 1 μM CTT, the controls with DMSO only. Every 2 h 25 spheroids were transferred to the sensor chip for impedance recording. For comparison the measured data were normalised: $\Delta Z = (Z_{\text{Spheroid}} - Z_{\text{Electrode}})/Z_{\text{Electrode}}$, where ΔZ is the resulting increase in electrode impedance caused by isolation of the uncovered electrodes ($Z_{\text{Electrode}}$) through a spheroid (Z_{Spheroid}). For $f = 133$ kHz the maximum relative increase in impedance magnitude compared to that of an empty cavity is plotted against the time of incubation with CTT. Bars represent the standard deviation of 3 independent experiments. $\star p < 0.05$.

stage (determined by dissociation and counting via Casy® Cell Counter System).

For comparison of treated and non-treated spheroids, the normalised impedance (ΔZ) at a single frequency (133 kHz) was plotted against time after treatment (Fig. 3), with ΔZ being the increase in electrode impedance caused by isolation of an uncovered electrode with a spheroid. CTT, an inhibitor of DNA Topoisomerase I (Pommier, 2006), was used to induce apoptosis in human melanoma spheroids. Cryosections of tumour spheroids revealed a slight but significant increase of cleaved, i.e. active caspase-3 in 1 μM CTT-treated melanoma spheroid cultures when compared to controls, i.e. an increase of $1.1 \pm 0.3\%$ caspase-3 positive cells per sphere at day 2, of $1.4 \pm 0.6\%$ at day 4, of $1.6 \pm 0.4\%$ at day 6, and of $2.3 \pm 0.4\%$ at day 8 *in vitro*. The controls remained at around $0.5 \pm 0.2\%$ for all states. Even after just 4 h ΔZ rose about 5% up to $40.4 \pm 4.5\%$ in spheroids that were treated with 1 μM CTT, whereas non-treated spheroids showed a value of $34.2 \pm 4.5\%$. This effect becomes even more evident 6 and 8 h after CTT treatment. *p*-Values for each point in time were determined with $p = 0.00316$ after 2 h, $p = 0.00580$ after 4 h, $p = 0.00031$ after 6 h and $p = 0.00001$ after 8 h ($n = 3$ independent experiments; Fig. 4a). The induction of apoptosis was confirmed by a TUNEL-Assay (data not shown).

The normalised impedance of these melanoma spheres increased compared to controls that displayed an average of around $34 \pm 5\%$. After 2 h ΔZ of treated spheres rose to $39.5 \pm 4.2\%$ ($p = 0.123$), to $40.4 \pm 4.5\%$ after 4 h ($p = 0.014$), to $47.2 \pm 5.0\%$ after 6 h ($p = 0.036$), and after 8 h *in vitro* ΔZ was $44.0 \pm 4.2\%$ ($p = 0.008$). *p*-Values were determined for $n = 3$ individual impedance measurements (Fig. 3).

In a second set of experiments we tested whether MCAs are suited for recording of action potentials of cardiac spheroids. Fig. 5a shows stable and continuous contractions of spheroids derived from neonatal rat cardiac myocytes. Electrical alterations caused by inward and outward currents have been measured between two electrodes of each cavity. Contractions have been visible not only on single cells but on the entire spheroid. After application of the specific Ca^{2+}-channel blocker Nifedipin (10^{-5} M) the formation of action potentials was completely eliminated.

Moreover, the 4-electrode configuration allows the monitoring of the position of spheroids in the cavities and to assess the electrode contact. With a switch for a programmed reading out spectra of all combinations of electrodes (six possible pairs) can be recorded individually (Fig. 6c). For a graphical interpretation color schemes (Fig. 6d) were created based on the impedance

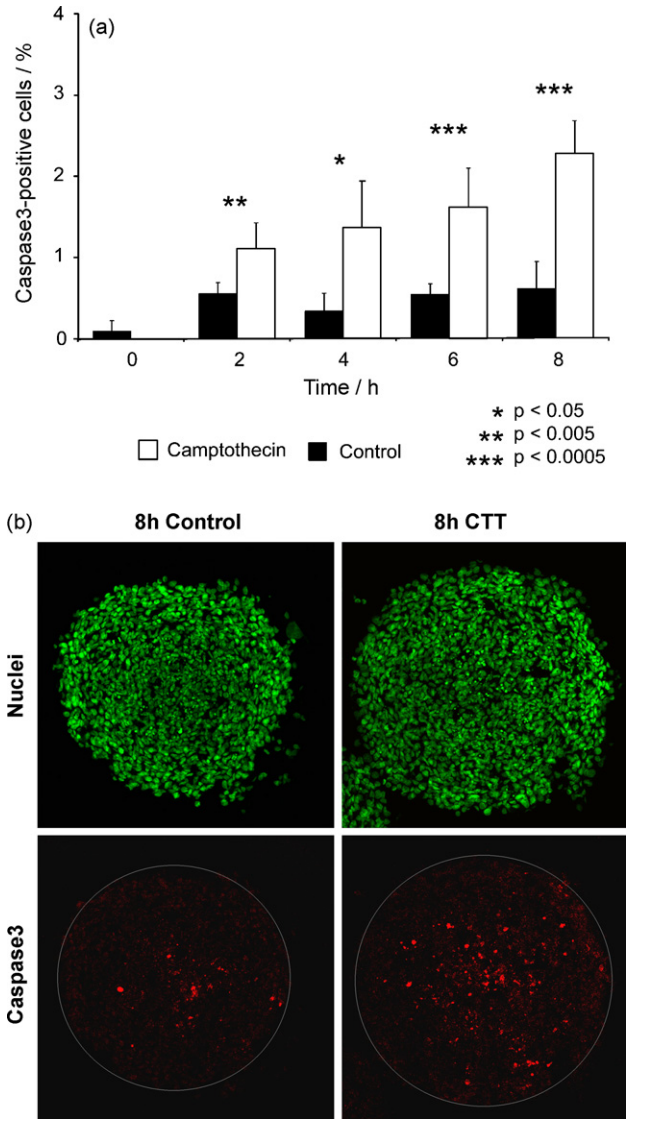

Fig. 4. (a) Increasing apoptosis rates in human melanoma spheroids after treatment with Camptothecin (CTT). The amount of apoptosis is quantified by 10 times calculating the ratio between caspase-3 positive cells and the total number of nuclei. $\star p < 0.05$, $\star\star p < 0.005$, $\star\star\star p < 0.0005$. (b) Histochemical staining of human melanoma spheroid cryosections. The number of caspase-3 positive cells (red) and nuclei (stained with Sytox green) indicates the increased amount of apoptotis (induced by CTT 8 h after treatment) compared to controls.

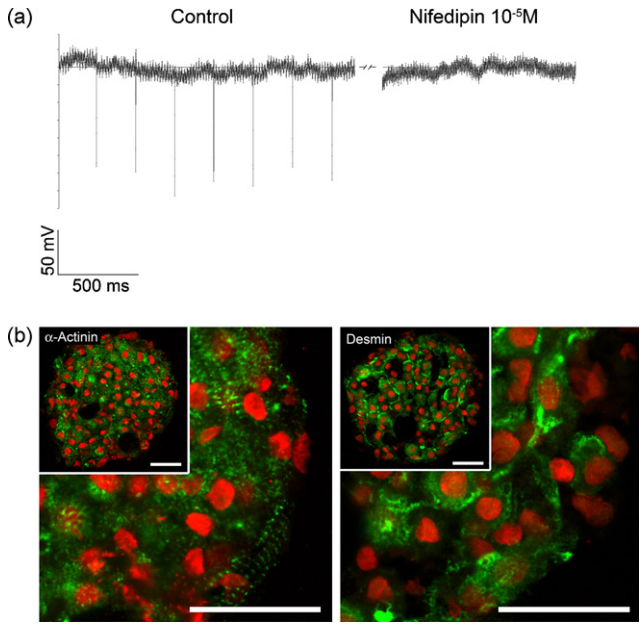

Fig. 5. (a) Extracellular potentials recorded from cardiomyocyte spheroids on the microcavity chip. Contraction rate was ~180 to 240 min^{-1}. With the specific Ca^{2+}-channel blocker Nifedipin contractions were completely stopped. (b) Histochemical staining of rat cardiomyocyte spheroid cryosections. Characterisation of the tissue is done by staining the specific marker proteins α-Actinin and Desmin. Nuclei (red) are stained with Sytox orange, bars = 100 μm.

data to give a spatial pattern of the signal distribution and thereby enables the observation of the positioning (Fig. 6d(1) and (2)) or optimum contact to every four electrodes (Fig. 6d(3)). For a high content screening and/or scale up of the parallel testing of various compounds, the MCA was completed with a multichamber cap (Fig. 6b). For the parallel testing of drug effects on spheroid cultures an adapter with either a 4-well unit (for the use of the 300 μm cavities) or 9-well unit (for using the three 400 μm and six 200 μm cavities) was developed and tested. The geometries of the conical chambers (3.3 mm × 3.3 mm at the bottom) correlate with the geometry of commercial 384-well plates. The cap was fixed by silicone to create individual measurement compartments with one cavity in each well on the array.

4. Discussion

The presented MCA has several advantages when compared to traditional impedance recordings of monolayer cultures (Pancrazio et al., 1999; Stett et al., 2003; El-Ali et al., 2006). For impedance analysis of monolayer cultures, most often a special coating of the surface with cell type specific adhesion molecules is necessary to improve cell or tissue adherence. Such coating is not compulsory for MCA-based impedance measurements, as a close contact between tumour spheroids and electrodes is already established when spheroids drop into the cavities. 3D systems demand 3D microstructures to be adequately analyzed by maintaining their shape and their properties during measurements.

Gravity causes an appropriate contact pressure that is sufficient for proper measurements. Measuring artefacts caused by any coating can be excluded since adhesion and growth inside the cavities is not intended. Spheroids cannot move during measurements since trapped in cavities of appropriate size. Its gravities are sufficient for that fixation. For spheroids of similar size comparable gravities/weight can be assumed, so the contact pressure and the contact area are similar for all compared spheroids. The system does not use complex hydrodynamic positioning or channels. A microscope and a micropipette (and the impedance measurement device) are enough to monitor and position 25 spheroids and record spectra in less than 10 min.

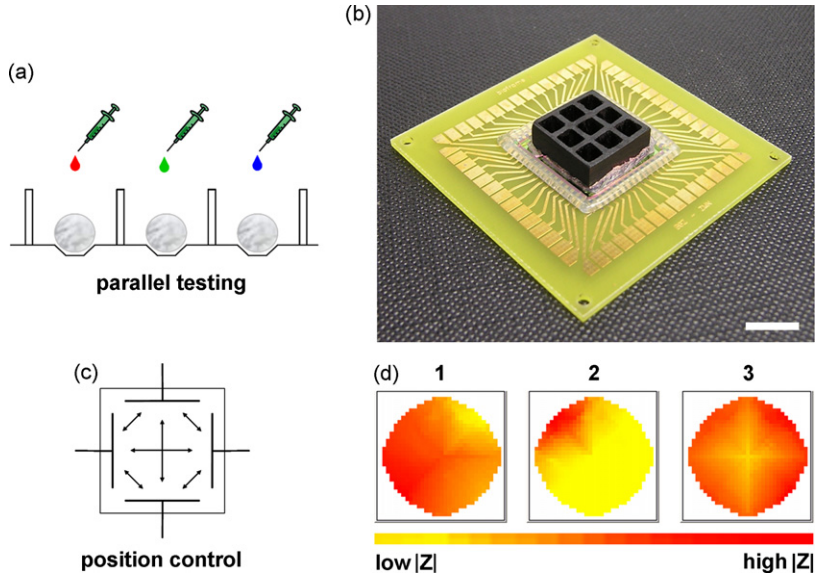

Fig. 6. (a) Schematic drawing to illustrate synchronous screening of different substances on one array (not to scale). (b) Photograph of a MCA with a multichamber cap. The adapter dimensions fit to 384-well geometry, a fixation on the MCA substrate was done using silicone, bar = 1 cm. (c) Schematic drawing of six possible pairs (arrows) of electrodes for identifying the spatial resolution of signals in every cavity. (d) Intensity distribution of impedance signals for determining the position of spheroids in the cavities. 1 and 2 = suboptimal positioning with high signal density on one side, 3 = central positioning with equal contact to every four electrodes.

The system is meant to be an acute test system for simple and fast positioning and monitoring of 3D spheroid cultures. The field of applications for the novel cavity-based biosensor provides pharmaceutical research with an effective screening tool for real-time high content drug screening tests that specify the effects of substances on three-dimensional *in vitro* tissues. An automated positioning (roboting system) is in development for real high throughput attempts.

Based on the observation that changes in impedance magnitudes occur at around 100 kHz and in agreement with previous studies (Kyle et al., 1999; Bartholoma et al., 2005), we assume that modified cell morphology, cell-to-cell interactions or the cell environment are the source of alterations in the dielectric properties of spheroids. In this context, our data are in accordance with a number of previous studies reporting that alterations in cell membranes (Paunescu and Helman, 2001), cytoskeleton (Moy et al., 1996) or formation of cell–cell contacts (Moy et al., 2000) can be measured in the β-dispersion range from 60 kHz to 5 MHz. The exact characteristic frequencies seem to be dependent on the cell/tissue type (data not presented here). Control experiments with porous inorganic sphere models indicate that signal intensity mainly depends on the permeability of the objects. For biological samples only data from one particular cavity are used for comparison. Furthermore, for all experiments ΔZ values are calculated and used for evaluation, so system parameters (parasitics) are identical and any effects can be suspected to be of biological origin.

For non-covered electrode pairs we found, as expected, different impedance spectra and phase angles for every cavity size depending on the geometries. So the decreasing capacities in larger cavities (lower phase angles) are displayed due to the fact that they have larger electrode surfaces and distances.

The unexpected slight increase of the impedance in CTT-treated melanoma spheres is reflecting that the cell density of the spheres might not have changed. Obviously the small amount of apoptotic (caspase-3 positive) cells did not influence the cellular package, cell–cell interaction and density of the entire melanoma spheroid.

In previous studies a significant and dramatic induction or increase of apoptosis in breast cancer spheroids could be detected by a decrease of the impedance or extracellular resistance R_{ext} (Thielecke et al., 2001; Bartholoma et al., 2005). In this study melanoma cell spheroids were investigated, these cells show other properties than breast cancer cells and their spheroids are differently organised compared to breast cancer spheres. The degree of CTT induced and mediated apoptosis was low and the cell density of the spheres (control vs. CTT treated) was not altered. According to nuclei staining of spheres and determination of the diameter and the amount of cells per dissociated sphere (Casy® Cell Counter System) the packing density of cells in the spheroids remained unaffected. Melanoma cells even seem to be more aggressive and proliferative. Effects and/or remodelling on or of the structure of the extracellular matrix might also cause an increase in the extracellular resistance. The impedance data could not reveal whether the uptake of CTT by melanoma cells was inefficient, i.e. the compound was exported via a multidrug resistance channel off the tumour cells. Limiting effects of drug penetration can also play a role for the distribution of a drug in the spheroid. Since spheroids usually have a core of non-proliferating cells and a shell of viable cells most of the effects of drugs are supposed to take place in the outer layers of cells. Recent experiments show morphological changes on the surface of drug treated spheroids. While treated spheroids have a smooth outside, controls are lightly rough. Those spheroids may have developed some sort of resistance mechanism that increases impedance due to an altered morphology. An induction of apoptosis in 3D tumours does not obligatory cause a disintegration of the tumour tissue although gene expression of the cell death molecule caspase-3 has been initiated and increased. Therefore, this low effect of apoptosis on the density of vital cells in a complex spheroid can be compensated by proliferation processes, i.e. morphological changes cannot be monitored or detected by molecular assays like caspase-3 expression. Thus, using our established tumour based biosensor in combination with bioimpedance spectroscopy we are able to show that a drug (CTT) induced apoptosis will not directly result in a disintegration and damage of a complex aggressive 3D *in vitro* melanoma tumour. This MCA enables the monitoring of the effects of chemotherapeutics on tumours and their morphological behaviour online within milliseconds omitting any manipulation and labelling. Unfortunately, there is no simple one-event – one-spectrum – correlation. To elucidate the exact molecular origin of any modulations in the spectra other influencing parameters have to be extracted one by one in the future and examined by a reliable equivalent circuit model.

Recordings of electrophysiological properties by different types of cardiomyocyte-based biosensors (Franks et al., 2007; Yang et al., 2007; Meyburg et al., 2006; Cheng et al., 2006), have several advantages, especially in comparison to classical patch clamp techniques. For instance, extracellular recording of field potentials by MCAs or FETs (Meyburg et al., 2006) are non-destructive techniques that allow long-term experiments of cardiac spheroids. The possibility of parallel measuring of alterations in membrane potentials simultaneously at multiple recording sites allows the use of the presented MCA for a semi-automated and non-invasive screening, especially with a view to the detection of ion channel associated diseases and to the testing of drugs regarding their effects and side effects in 3D cellular cultures.

Another striking advantage, especially when compared to single-use chip systems is that all system components of the sensor chip were selected according to specific requirements such as long-term mechanical and thermal stability. The MCAs can be used repeatedly, sterilized by autoclaving or cleaned by ultrasonic, tensides, or ethanol. Since the measuring system is biocompatible, non-destructive, long-term experiments and subsequent histochemical or molecular biological analyses can be carried out without any difficulty. The demonstrated multiwell cap with four or nine chambers, respectively, is a helpful upgrade for a parallel and synchronous testing of drugs on one MCA. Scaling up the system with a combination of suitable well and cavity dimensions to larger formats than those presented here

should be possible. Moreover, electric interactions of conductors on the chip surface are minimized once separate wells are used for analyses of cavity trapped spheroids.

The 4-electrode configuration can be used to cross-check the results of one 2-point measurement with the remaining two electrodes. When adding the signals from kitty-corner electrodes, the spheroid position inside a cavity can be assessed. Such a position control can be performed online by illustrating the distribution of signals. This becomes important in the case of the monitoring of electrogenic cardiomyocytes where contractions lead to deformation of the spheroids and thereby to alterations of the contact area between cells and electrodes.

The development of the next generation of sensor chips is in progress. Since the sensor chip presented in this study is a prototype, improvements of the system have to be considered. Refinements in electrode and conductor design for 4-point measurements will be made to limit parasitic influences of conductors and the measurement system itself. An optimised geometry would allow for the analysis of a larger range of spheroid sizes.

Another main aspect will be the use of transparent substrate materials for better microscopic applicability. Future systems could be miniaturised to make them suitable for single cell analysis. Positioning and controlling of the contact pressure can be enhanced by application of vacuum through integrated suction channels ($\sim$5 to 10 μm in diameter) on the bottom of each cavity. Compared to chip systems that use microfluidics (Yang et al., 2007; Cheng et al., 2006) for positioning of particles in vertical or horizontal channels, the present cavity system is less complex. A combination of both approaches can be a further optimisation when thinking of miniaturisation and integration of channels for the sorting of particles (spheroids or single cells) before carrying out any analyses.

Acknowledgements

This work is funded by the German Research Foundation (DFG; SFB610, Z5 Rob.), the European Community (Project “Cardioworkbench”, STREP no. 018671), and the European Fond for Regional Development (“Tumorsensor”, AZ: 4-0123.55-20-0361-04/13). For helpful suggestions during proof-reading we would like to thank Prof. Kathryn Nixdorff (TU Darmstadt).

References

Bartholoma, P., Impidjati, Reininger-Mack, A., Zhang, Z., Thielecke, H., Robitzki, A., 2005. J. Biomol. Screen. 10 (7), 705–714.
Cheng, W., Klauke, N., Sedgwick, H., Smith, G.L., Cooper, J.M., 2006. Lab. Chip. 6 (11), 1424–1431.
El-Ali, J., Sorger, P.K., Jensen, K.F., 2006. Nature 442 (7101), 403–411.
Franks, W., Tosatti, S., Heer, F., Seif, P., Textor, M., Hierlemann, A., 2007. Biosens. Bioelectron. 22 (7), 1426–1433.
Kunz-Schughart, L.A., Kreutz, M., Knuechel, R., 1998. Int. J. Exp. Pathol. 79 (1), 1–23.
Kyle, A.H., Chan, C.T.O., Minchinton, A.I., 1999. Biophys. J. 76, 2640–2648.
Layer, P.G., Robitzki, A., Rothermel, A., Willbold, E., 2002. Trends Neurosci. 25 (3), 131–134.
Meyburg, S., Goryll, M., Moers, J., Ingebrandt, S., Böcker-Meffert, S., Lüth, H., Offenhäusser, A., 2006. Biosens. Bioelectron. 21 (7), 1037–1044.
Moy, A.B., Van Engelenhoven, J., Bodmer, J., Kamath, J., Keese, C., Giaever, I., et al., 1996. J. Clin. Invest. 97, 1020–1027.
Moy, A.B., Winter, M., Kamath, A., Blackwell, K., Reyes, G., Giaever, I., et al., 2000. Am. J. Physiol. Lung Cell. Mol. Physiol. 278, L888–L898.
Pancrazio, J.J., Whelan, J.P., Borkholder, D.A., Ma, W., Stenger, D.A., 1999. Ann. Biomed. Eng. 27, 697–711.
Paunescu, T.G., Helman, S.I., 2001. Biophys. J. 81, 852–866.
Pommier, Y., 2006. Nat. Rev. Cancer 6 (10), 789–802.
Reininger-Mack, A., Thielecke, H., Robitzki, A., 2002. Trends Biotechnol. 20, 56–61.
Rothermel, A., Kurz, R., Ruffer, M., Weigel, W., Jahnke, H.G., Sedello, A.K., Stepan, H., Faber, R., Schulze-Forster, K., Robitzki, A.A., 2005. Cell Physiol. Biochem. 16 (1–3), 51–58.
Stett, A., Egert, U., Guenther, E., Hofmann, F., Meyer, T., Nisch, W., Haemmerle, H., 2003. Anal. Bioanal. Chem. 377 (3), 486–495.
Thielecke, H., Mack, A., Robitzki, A., 2001. Biosens. Bioelectron. 16 (4–5), 261–269.
Yang, M., Lim, C.C., Liao, R., Zhang, X., 2007. Biosens. Bioelectron. 22 (8), 1688–1693.